APPLIED AND ENVIRONMENTAL MICROBIOLOGY, Aug. 1997, p. 3261–3267 Vol. 63, No. 8
0099-2240/97/$04.00+0

Quantitative Fluorescence In Situ Hybridization of *Aureobasidium pullulans* on Microscope Slides and Leaf Surfaces

SHUXIAN LI, RUSSELL N. SPEAR, AND JOHN H. ANDREWS*

Department of Plant Pathology, University of Wisconsin, Madison, Wisconsin 53706

Received 25 February 1997/Accepted 29 May 1997

A 21-mer oligonucleotide probe designated Ap665, directed at the 18S rRNA of *Aureobasidium pullulans* and labelled with five molecules of fluorescein isothiocyanate, was applied by fluorescence in situ hybridization (FISH) to populations of the fungus on slides and apple leaves from growth chamber seedlings and orchard trees. In specificity tests that included Ap665 and a similarly labelled universal probe and the respective complementary probes as controls, the hybridization signal was strong for Ap665 reactions with 12 *A. pullulans* strains but at or below background level for 98 other fungi including 82 phylloplane isolates. Scanning confocal laser microscopy was used to confirm that the fluorescence originated from the cytoplasmic matrix and to overcome limitations imposed on conventional microscopy by leaf topography. Images were recorded with a cooled charge-coupled device video camera and digitized for storage and manipulation. Image analysis was used to verify semiquantitative fluorescence ratings and to demonstrate how the distribution of the fluorescence signal in specific interactions (e.g., Ap665 with *A. pullulans* cells) could be separated at a given probability level from nonspecific fluorescence (e.g., in interactions of Ap665 with *Cryptococcus laurentii* cells) of an overlapping population. Image analysis methods were used also to quantify epiphytic *A. pullulans* populations based on cell number or percent coverage of the leaf surface. Under some conditions, leaf autofluorescence and the release of fluorescent compounds by leaves during the processing for hybridization decreased the signal-to-noise ratio. These effects were reduced by the use of appropriate excitation filter sets and fixation conditions. We conclude that FISH can be used to detect and quantify *A. pullulans* cells in the phyllosphere.

There are numerous indirect and direct methods to detect, monitor, and quantify strains or species in various microbial communities; the advantages and disadvantages of each have been discussed previously (3, 17, 30). Fluorescence in situ hybridization (FISH) is a relatively recent and powerful innovation combining the specificity inherent in nucleic acid sequences with the sensitivity of detection systems based on fluorochromes. FISH originated in medicine and developmental biology for the localization of particular DNA sequences in mammalian chromosomes (36, 37) and subsequently has been applied primarily in environmental bacteriology (1, 8) and to a lesser extent in protist ecology (27). To date, the use of FISH in fungal biology has been limited to genetic studies (23, 38) and to a documentation of the potential uses of the method (10, 16).

In brief, FISH involves the detection of DNA or RNA sequences in cells or tissues by the use of RNA or DNA probes, typically of 17 to 300 bases, labelled directly or indirectly with fluorochromes (22, 35). Under appropriate reaction conditions, complementary sequences in the probe and target cell anneal, and the site of probe hybridization is detected by fluorescence microscopy (2, 16). In environmental microbiology studies, rRNA is a common target for probes because ribosomes are plentiful (though they vary in number with growth rate) and because selection of particular regions of the rRNA molecule enables phylogenetic specificity to be varied from the universal to the subspecies level (4, 10, 16, 39). In general, fluorescence has been judged qualitatively, though occasionally signal strength has been quantified by image analysis (21, 31) or flow cytometry (4, 10, 39).

Our long-term goals are (i) to quantify the roles of birth, death, immigration, and emigration in the population biology of a yeast-like fungus, *Aureobasidium pullulans* (de Bary) Arnaud, on leaf surfaces and (ii) to map, temporally and spatially, the epiphytic colonization patterns of *A. pullulans*. These objectives necessitate the ability to distinguish and enumerate specifically *A. pullulans* cells within the leaf surface community by an in situ method that preserves microbe-substratum (microenvironmental) relationships (12). The ecology of *A. pullulans* is of interest because this ubiquitous organism (14) is one of the few fungi that actively grows on living leaves (7) and because it has potential as a biological control agent of plant pathogens (6). The actively growing morphotypes of *A. pullulans* are primarily blastospores and swollen cells, though most strains of the fungus can also produce, to some extent, chlamydospores, hyphae, and pseudohyphae under culture conditions (7, 14). The method of choice to accomplish our goals appeared to be FISH, and we report here that it can be used effectively in the study of phylloplane microbiology as represented by our model system. Development of the oligonucleotide probe is described elsewhere (26), and brief, preliminary reports on the FISH results also have appeared (24, 25).

MATERIALS AND METHODS

Cell cultures and growth conditions. The sources and strain designations of the fungi have been reported previously (26). For long-term storage, cells were suspended in 15% glycerol and held at −80°C until used. Working cultures in routine use were grown on potato dextrose agar (Difco, Detroit, Mich.) at 25 to 28°C and transferred at 1- to 2-week intervals. For experiments, single colonies were inoculated into flasks of yeast-peptone-glucose broth and incubated as shake cultures at 25°C. Exponentially growing cells were harvested after 18 to 20 h, washed twice with phosphate-buffered saline (0.05 M $NaPO_4$, 0.15 M NaCl [pH 7.2]), and fixed either with freshly prepared depolymerized 3% paraformal-

* Corresponding author. Mailing address: Department of Plant Pathology, University of Wisconsin-Madison, 1630 Linden Dr., Madison, WI 53706-1598. Phone: (608) 262-9642. Fax: (608) 263-2626. E-mail: JHA@plantpath.wisc.edu.

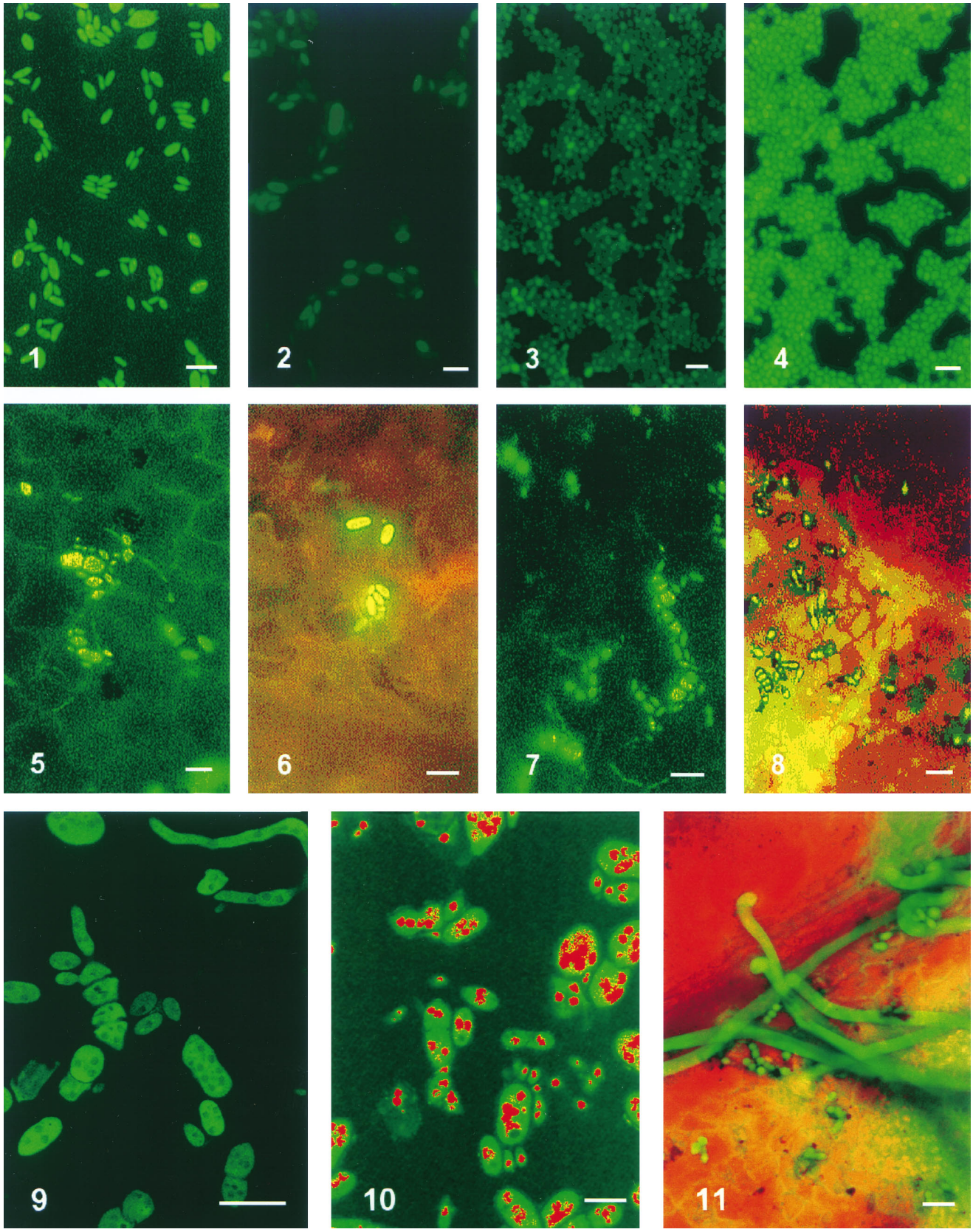
1
2
3
4
5
6
7
8
9
10
11

FIG. 1–11. Epifluorescence micrographs of *A. pullulans* and other fungi on microscope slides (Fig. 1–4, 9 and 10) or on apple leaf surfaces (Fig. 5–8 and 11) based on in situ hybridization results with FITC-labelled, *A. pullulans*-specific (Ap665), complementary control (non-Ap665), or universal (U519) probes. Bars, 10 μm.

FIG. 1. *A. pullulans* and probe Ap665.

FIG. 2. *A. pullulans* and the corresponding negative control, probe non-Ap665.

FIG. 3. Specificity of probe Ap665 demonstrated by the weak signal from hybridized cells of the yeast *C. laurentii.*

FIG. 4. *C. laurentii* showing a strong signal when hybridized with the positive control, universal probe U519.

FIG. 5. *A. pullulans* on the adaxial phylloplane of an apple seedling; probe Ap665.

FIG. 6. *A. pullulans* on the adaxial phylloplane of an orchard tree; probe Ap665. Background color results from use of a dual-emission filter allowing both the green FITC signal from *A. pullulans* and the red-tan autofluorescence of the leaf to be seen simultaneously. Autofluorescent background and extractable compounds from the leaf cause the FITC signal to shift from green to more yellow.

FIG. 7. Fungal cells on the adaxial phylloplane of an apple seedling; universal probe U519.

FIG. 8. Fungal cells on the adaxial phylloplane of an orchard tree. The dual-filter set was as in Fig. 6, and universal probe U519 was used. Background color is due to red-tan leaf autofluorescence combined with some hybridization with rRNA in the leaf tissue (lower left) by the universal probe.

FIG. 9 and 10. SCLM of *A. pullulans* cells without (Fig. 9) or with (Fig. 10) counter-staining by PI following hybridization with probe Ap665.

FIG. 9. A pseudocolored image collected in the green (FITC) channel showing that the hybridization signal originates from the cytoplasmic matrix; the dark circular areas represent nuclei or vacuoles separable by the nucleic acid-specific stain PI, which was used for Fig. 10, where nuclei appear red.

FIG. 10. A merged, pseudocolored image collected in green and red channels of five optical sections, each 0.5 μm thick. Yellow margins represent overlap between channels.

FIG. 11. SCLM of the abaxial phylloplane from an orchard tree, probe Ap665. Cells and trichomes appear green. This is a merged image of 20 optical sections, each 1.0 μm thick, displayed in two pseudocolored channels, red and green.

dehyde in phosphate-buffered saline or with methanol-acetic acid (3:1 [vol/vol]) overnight at 4°C. The filamentous fungi used in specificity tests (described below) were grown by standard methods on potato dextrose agar, with the exception of *Blastocladiella emersonii*, which was grown as described by Soll et al. (34). The sporulating thalli were removed from plates either en masse by tweezers, in which case the colonies were placed directly into the fixative, or by flooding the agar surface with distilled water and scraping the colonies with a rubber policeman. Following fixation, the paraformaldehyde-fixed cells were washed twice for 10- to 20-min intervals in diethyl pyrocarbonate (0.1%)-treated, autoclaved distilled water (DW) (22) and stored at −20°C in 70% ethanol until hybridization. The methanol-acetic acid-fixed cells were instead washed twice in 70% ethanol prior to storage as described above.

Fungi on apple leaves. FISH was performed on apple leaf tissue from two sources. First, apple seedlings were grown under standard conditions in growth chambers (6), spray-inoculated with *A. pullulans* ATCC 30393 at 10^6 cells · ml^{-1}, and incubated for 7 to 10 days. Second, apple (*Malus* × *domestica* Borkh. cv. McIntosh) or crab apple (*Malus* × *sublobata* [Dipp.] Rehd.) leaves were harvested from trees at the West Farm Experiment Station, Madison, Wis. or on the University of Wisconsin-Madison campus periodically during the summers of 1995 and 1996. When field leaves were not extensively colonized by *A. pullulans*, microbial growth was promoted by misting them with water, followed by incubation in moist chambers at 23 to 25°C for 3 to 7 days. This facilitated locating the fungus at densities necessary to test the probes and automated enumeration by image analysis methods. Disks (5 mm in diameter) were punched from leaves with a cork borer, and the tissue was fixed and then stored in 70% ethanol at −20°C as described above for cell cultures.

Oligonucleotide probes and labelling. The following probes were used: Ap665, an rRNA-targeted oligonucleotide probe (26) designed for *A. pullulans* (5′-TTC GTT TAG TTA TTA TGA ATC-3′); U519, a universal oligonucleotide (18) complementary to a sequence of the 16S-like rRNA in all known organisms (5′-GAA TTA CCG CGG CTG CTG-3′); and the corresponding complementary probes non-Ap665 (5′-GAT TCA TAA TAA CTA AAC GAA-3′) and non-U519 (5′-CAG CAG CCG CGG TAA TTC-3′). Since they were complementary to the first two probes, i.e., rRNA-like as opposed to being complementary to rRNA (18), the latter probes served as a negative control for nonspecific binding. All probes were synthesized and labelled with fluorescein isothiocyanate (FITC) by CLONTECH Laboratories (Palo Alto, Calif.) using a symmetric branching phosphoramidite. Each probe had four FITC molecules on the 5′ end and one FITC molecule on the 3′ end, appropriately spaced to reduce quenching. All probes were stored dry in the dark at −20°C.

Whole-cell hybridization. Fixed cells from ethanol storage were washed twice in diethyl pyrocarbonate-treated DW, placed in 10-μl aliquots on Superfrost-Plus slides (Fisher Scientific, Pittsburgh, Pa.), and air dried. Leaf disks were hydrated at 20-min intervals through 70, 50, and 30% ethanol, followed by hydration through DW (twice), in microtiter plates.

For prehybridization, 10 μl of hybridization solution (HS) (see below) without the probe was added to slides, which were incubated at 37°C for 30 min to 1 h under optimized conditions for our system in 5× SSC-saturated humidity chambers (1× SSC is 0.15 M NaCl plus 0.015 M sodium citrate) (22, 35). Leaf disks were incubated similarly, but in 25 μl of HS in capped microcentrifuge tubes. HS was prepared from a 2× stock solution (Sigma, St. Louis, Mo.); the final composition was 5× SSC, 1× Denhardt's solution, 100 μg of sheared DNA ml^{-1}, 10% dextran sulfate, and deionized formamide (Sigma; 50% for probes U519 and non-U519; 15% for probes Ap665 and non-Ap665). For hybridization, slides or leaf samples were incubated in darkness at 37°C for from 3 h to overnight in HS with 50 ng of fluorescent probe under humidified conditions as described above. Following hybridization, slides or leaf samples were washed once (10 min) in 1× SSC and then twice (10 min each) in 0.1× SSC, mounted in antifade medium (VectaShield; Vector, Burlingame, Calif.), and observed immediately or after storage at −20°C.

As controls, each batch of slides or leaf samples processed for hybridization included labelled oligonucleotides complementary to the probes, theoretically incapable of hybridizing with the rRNA, as noted above, and material from which the probe was omitted (autofluorescence controls). Additionally, specificity was tested periodically by mixing unlabelled and labelled probes in competitive binding assays at ratios of labelled to unlabelled probe of 1:10 and 1:50 and observing specimens for diminished fluorescence. Preliminary control experiments were also done to verify the subcellular location of the FITC signal. Scanning confocal laser microscopy (SCLM; see below) facilitated separation of the cytoplasmic matrix from nuclei and vacuoles, which in turn were separable by digesting hybridized cells with RNase A (10 μl/ml) for 1 h at 37°C and counterstaining with the nucleic acid-specific stain propidium iodide (PI) (5 μg/ml) for 20 min prior to microscopy (19).

Specificity tests with heterologous fungi. The specificity of the Ap665-FITC probe was evaluated for all 12 *A. pullulans* strains and for the 98 other fungal isolates assayed earlier by Southern blots (26) and selected on the basis of the phylogenetic, taxonomic, and ecological criteria discussed previously (26). Fixed, washed blastospores (yeasts) or conidia and hyphae (filamentous fungi) were suspended at a concentration sufficient to allow 500 to 700 propagules to be seen at ×400 magnification. Teflon-printed, 12-well, glass microscope slides (Electron Microscopy Sciences, Fort Washington, Pa.) were dipped in gelatin-chrome alum adhesive (20), drained on filter paper, and dried at 37°C. A slide consisted of 10-μl drops of spores from each of 10 fungal isolates and two control strains, *A. pullulans* ATCC 90393 and *Rhodotorula glutinis* ATCC 1091, added separately to the wells and allowed to air dry. The procedure was repeated for a total of five slides for each batch of test isolates. Each slide received a different treatment as follows: One slide from each set was subjected to the in situ hybridization protocol without the probe (autofluorescence control); the remaining four slides were hybridized with either Ap665-FITC, non-Ap665-FITC, U519-FITC, or non-U519-FITC. Fluorescence intensity was rated semiquantitatively by eye on a scale of − to ++++, where − represented no detectable fluorescein response (autofluorescence only) and ++++ was an intense green-yellow FITC signal. Each treatment was replicated once within an experiment, and the experiment was repeated once.

The above subjective fluorescence rating scheme was validated by quantitative image analysis methods with representative fungi. For example, cells of *A. pullulans* and *Cryptococcus laurentii* were hybridized with probes Ap665 and non-Ap665, and specimens that had not been hybridized were included as autofluorescence controls. Digital images of the fungal population on each slide, collected under identical conditions of camera gamma, brightness, and contrast, were analyzed for fluorescence intensity distribution. A color threshold was set to include all cells in the field based on the green-yellow emission color of fluorescein (29). Local image smoothing was applied to correct for uneven background illumination without affecting the objects included in the threshold (29). From this processed image, average color intensity values were determined for each cell by use of Optimas 5.2 image processing software (Optimas Inc., Bothell, Wash.) and were stored in an Excel 5 (Microsoft Corp., Redmond, Wash.) spreadsheet. Cell fluorescence intensity data were analyzed with MiniTab version 11.0 software (Minitab, Inc., State College, Pa.) and plotted as histograms of average cell fluorescence intensity (the sum of the pixel intensity values of the cell divided by the number of pixels) versus the percentage of the cell population, by use of SigmaPlot version 2.0 software (Jandel Scientific, San Rafael, Calif.). For reasons discussed later, the lower 2.5th percentile of the fluorescence distribution of *Aureobasidium* with probe Ap665 was chosen as the cutoff limit between specific and non-specific hybridization signals.

TABLE 1. The two major reaction patterns of *Aureobasidium pullulans* and heterologous fungi based on FISH with four oligonucleotide-FITC probes

Species[a] exhibiting probe reaction pattern[b]:	
A	B
Alternaria alternata NRRL 5255	*A. pullulans* ATCC 28998
Aspergillus nidulans FGSC 4[c]	*A. pullulans* WF1
Blastocladiella emersonii ATCC 22665[d]	*A. pullulans* WF2
Candida parapsilosis (1 isolate)[e]	*A. pullulans* var. *pullulans* CBS 704.76
Cladosporium cladosporioides NRRL 20632	*A. pullulans* ATCC 90393
Cladosporium herbarum NRRL 2175	*A. pullulans* NRRL 12779
Colletotrichum gloeosporioides JHA S19-3	*A. pullulans* NRRL Y2567
Cryptococcus albidus (10 isolates)[e]	*A. pullulans* ATCC 48168
C. laurentii (29 isolates)[e]	*A. pullulans* var. *melanigenum* ATCC 12536
C. laurentii NRRL 2536	*A. pullulans* var. *melanigenum* CBS 210.65
Hormonema dematioides CBS 116.29	*A. pullulans* var. *pullulans* CBS 584.75
Leucostoma persoonii ATCC 62911	*A. pullulans* var. *pullulans* ATCC 11942
Neurospora crassa FGSC 2490	
Ophiostoma ulmi JHA 82	
Penicillium chrysogenum NRRL 807	
Penicillium notatum ATCC 9179	
Podospora anserina FGSC 6710	
Rhodotorula glutinis (11 isolates)[e]	
Rhodotorula minuta (10 isolates)[e]	
Rhodotorula rubra (9 isolates)[e]	
Rhodotorula rubra NRRL 1592	
Rhodotorula sp. (10 isolates)[e]	
Sporobolomyces holsaticus NRRL 17285	
Sporobolomyces sp. (1 isolate)[e]	
Unknown yeast (1 isolate)[e]	

[a] NRRL, Northern Regional Research Lab, Peoria, Ill.; ATCC, American Type Culture Collection, Rockville, Md.; CBS, Centraalbureau voor Schimmelcultures, Baarn, The Netherlands; FGSC, Fungal Genetics Stock Center, Kansas City, Kans.; WF1 and WF2, field isolates from Madison, Wis.; JHA, J. H. Andrews' collection, Madison, Wis.

[b] Except where noted otherwise, reaction patterns are based on hybridization signals from blastospores (yeasts) or conidia and hyphae (filamentous fungi). Negative (−) reactions include categories − and +/− on the semiquantitative scale; positive (+) reactions include categories from + to ++++ on the semiquantitative scale. See also Fig. 14. Probe reaction pattern A is as follows: Ap665, −; non-Ap665, −; U519, +; non-U519, −. Probe reaction pattern B is as follows: Ap665, +; non-Ap665, −; U519, +; non-U519, −.

[c] Morphotypes examined: hyphae, conidial heads, asci, ascospores, and Hülle cells. The reaction pattern noted applies to all morphotypes except ascospores (strong red autofluorescence), for which no signal from probe U519 was detectable.

[d] A fungus-like chytrid classified variously with the fungi or in the kingdom *Protista*. The reaction pattern is based on an examination of rhizoids, sporangia, and encysted zoospores. The culture was provided by D. Sonneborn.

[e] From the apple phylloplane (26).

Microscopy and image analysis. Specimens were examined with a BX-60 microscope (Olympus America Inc., Lake Success, N.Y.) equipped for epifluorescence with an HBO 100-W mercury arc lamp. Filters used were either an Olympus NIB narrow-excitation FITC set or the dual-filter set for FITC and Texas Red in the Olympus U83000 FISH filter set. The NIB set consisted of an exciter (Ex) filter (470 to 490 nm), a dichroic (Dichro) mirror (505 nm) and an emission (Em) filter (515LP). The dual-filter set specifications for FITC were as follows: Ex, 475 to 505 nm; Dichro, 500 to 545 nm; Em, 505 to 540 nm. Those for Texas Red were as follows: Ex, 563 to 598 nm; Dichro, 600 nm; Em, 584 to 620 nm. The dual set contrasted the specific green-yellow fluorescence of FITC against the red autofluorescence of chlorophyll in the leaf. Images were recorded with a cooled charge-coupled device video camera (DEI-470; Optronics Engineering, Goleta, Calif.) and were converted from an analog to a digital format (digitized) with a Targa +64 frame grabber (Truevision, Indianapolis, Ind.) controlled by the Optimas processing software running on a 486/80-MHz personal computer. The digitized images were stored as 24-bit red-green-blue tagged-image format files on 230-megabyte magneto-optical disks. SCLM was conducted with an MRC 600 unit (Bio-Rad, Hercules, Calif.) equipped with an Ar ion laser (excitation wavelength, 488 nm). FITC filters were used to examine hybridized cells on slides and leaves; the dual K1/K2 filter set (capable of simultaneously exciting and imaging rhodamine and fluorescein) was used for hybridized cells on slides that had been counterstained with PI. The resulting image sets were stored on optical media prior to processing. The confocal images were merged and pseudocolored with the Bio-Rad software supplied with the microscope or the program Confocal Assistant, version 3.10 (11). Final image adjustment for color printing was done with Adobe Photoshop software, version 3.05 (Adobe Systems, Inc., Mountain View, Calif.).

Image analysis of *A. pullulans* populations on leaves was conducted as follows. Naturally infested or spray-inoculated McIntosh apple leaves were fixed in paraformaldehyde and hybridized with probe Ap665, and digital images were collected as described above. Images in the red-green-blue-color format were converted to 8-bit (256-gray-level) form, and a region of interest (ROI) was selected to encompass an area in clear focus. This ROI was cut from the original image and pasted to form a new image frame. Thresholds were set to include hybridized cells and to exclude leaf structures and any cells that did not fluoresce. Joined cells were separated visually by the use of binary morphology operations of sequential erosion and nonmerging dilation (29). Cells were outlined by the outline command and filled by the fill command (29), the image was converted to a binary (B/W) image, the filled cells were counted, and areas were determined from stored calibration parameters. The total area of the selected ROI also was determined. From these values the percent area coverage was determined by the following equation: percent cell coverage = (area of cell cover/area of ROI) × 100.

RESULTS AND DISCUSSION

On microscope slides, blastospores and swollen cells of all 12 *A. pullulans* strains produced strong green-yellow fluorescence when exposed to the labelled Ap665 probe (Fig. 1). All cells stained positive, i.e., with an intensity of at least +, and >90% were rated as +++ to ++++. Samples processed without the hybridization step (autofluorescence controls) or hybridized with probe non-Ap665 (nonspecific binding controls) were uniformly negative (−) or dim (+/−), respectively (Fig. 2). Hyphae also hybridized with Ap665 (see confocal results below), and pigmented, thick-walled chlamydospores produced a faint but detectable fluorescence signal (+) (data not shown). Thus, all life cycle forms of *A. pullulans* can be detected by FISH, though some morphotypes are more readily visible than others. Further research on hybridization or permeation and decolorization protocols will be needed to determine an optimal regimen for chlamydospores.

Overall, there were two classes of FISH results based on the microscope slide assays with the four labelled probes. In one category (pattern A, Table 1; Fig. 3 and 4), the outcome was positive for the universal probe, which was used as a positive control for the occurrence of detectable sequences, but negative for non-U519, Ap665, and non-Ap665 probes. This trend was manifested by all the heterologous fungi (82 phylloplane isolates and 16 species from culture collections) (Table 1). Interestingly, *Hormonema dematioides*, which is taxonomically very similar if not identical to *A. pullulans* (15), did not react with the probe. In the other category (pattern B, Table 1), the outcome was positive for Ap665 and U519, but negative for non-Ap665 and non-U519. This trend was exhibited by all 12 *A. pullulans* strains tested. Based on these trials, we conclude that Ap665 is at least sufficiently specific for *A. pullulans* to be used in FISH protocols to detect the organism in its leaf surface habitat. These FISH results confirm and extend our earlier specificity data based on Southern blot hybridizations (26).

Ap665 hybridized with *A. pullulans* on leaves from apple seedlings grown under controlled conditions in growth chambers (Fig. 5) or from trees outdoors (Fig. 6). Under similar circumstances, the fluorescently labelled U519 probe hybridized, as expected, with diverse microbes on the phylloplane (Fig. 7 and 8). Controls used for the microscope slide experiments were again negative. Optical sectioning by SCLM of probed cells stained subsequently with PI (19) confirmed the

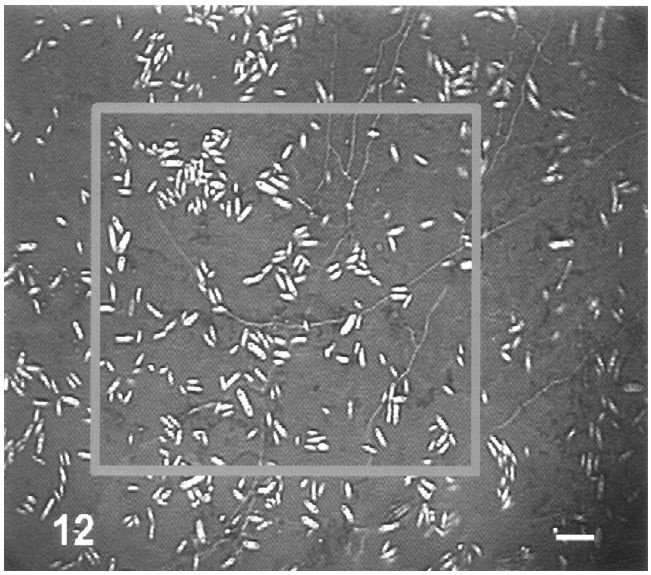

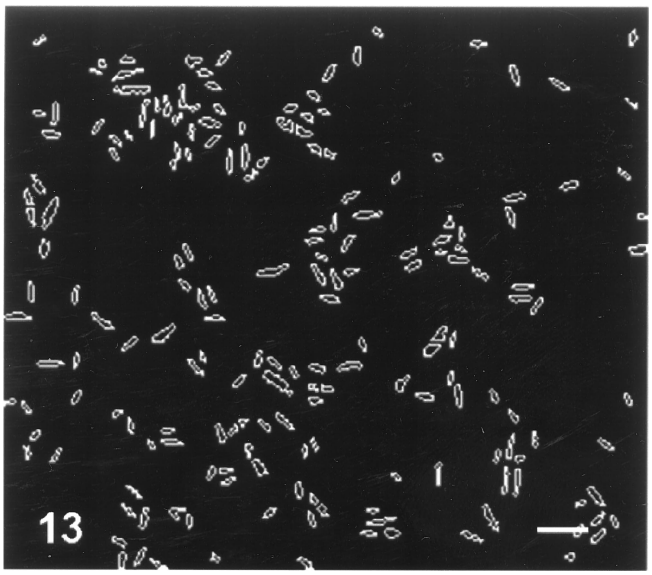

FIG. 12 and 13. Adaxial phylloplane of an apple seedling with applied *A. pullulans* cells hybridized in situ with probe U519.

FIG. 12. Typical view (8-bit image) of an epiphytic population as seen at low magnification (×20 objective) used for enumeration by image analysis; the ROI is demarcated by the square.

FIG. 13. The ROI as a 1-bit image after thresholds were set to include the hybridized cells and exclude as much background as possible. A binary fill filter has been used which renders cells white on a black background and facilitates quantification based on area of *A. pullulans* coverage (6,776 μm^2), area of leaf surface within the ROI (135,338 μm^2), percent area coverage (5%), or total cell number (229).

general cytoplasmic distribution of label and showed that it was absent from vacuoles (Fig. 9) and nuclei (Fig. 10). These results are consistent with the expectation that ribosomes are the target and support other lines of evidence from controls noted above that staining is specific. Because of its ability to reconstruct multiple in-focus image planes, SCLM was also valuable in viewing microbes on the contoured phylloplane, especially where colonized trichomes projected from the surface of epidermal cells (Fig. 11).

Our work demonstrates the potential applicability of quantitative image analysis in two contexts. First, it was possible to accurately enumerate cells of *A. pullulans* at natural and artificially elevated densities (at least up to 5%; see Fig. 12 and 13) on leaf surfaces. The data can be expressed in various forms such as area coverage, percent coverage, and cell number (Fig. 12 and 13) or cell size distribution (data not shown). Image analysis would not be accurate in situations where cells are stacked vertically, but this was not the case here. Multilayered biofilms would rarely, if ever, occur in fungal communities on terrestrial vegetation in temperate zones. Image analysis of leaf surfaces is best done on gray-scaled images because autofluorescence of the underlying leaf makes color thresholding of the image difficult. The selection of flat, in-focus ROIs is important to allow both cell separation filtering and proper edge detection. The problem of out-of-focus areas in specimens can be solved either by using merged image sets from confocal microscopy (13, 40) or by deconvolution techniques (33). We do not address here issues related to sampling (e.g., number of cells and number of ROIs required for statistical validity), which are under study. Finally, measurements of binary processed images, while useful for spatial measurements (area, coverage counts, and shapes), cannot be used for intensity determinations.

The second context for image analysis relates to analyzing the distribution of signal intensities from a population of interest (represented by *A. pullulans* cells) and discriminating it from another, morphologically similar, overlapping population (represented by *C. laurentii* cells) (Fig. 14). In principle, the dual objectives are to include all members of the target population and none of the nontarget population, but both goals cannot be met simultaneously. Stated differently, this means that one can choose either to be very certain that a brightly fluorescing cell is *A. pullulans* while recognizing that some dim *Aureobasidium* cells will be classified as *Cryptococcus* or that all cells of *Aureobasidium* (along with, erroneously, many *Cryptococcus* cells) indeed have been designated as *Aureobasidium*, but not both. The location of the threshold between the two populations will be set by the researcher's weighting of the two forms of error (failing to include legitimate *Aureobasidium* cells or declaring *Cryptococcus* cells to be *Aureobasidium*), the extent of overlap of the populations, and their prevalence in nature.

As a first approximation based on comparisons with the autofluorescence and non-AP665 controls, we chose as lower bounds on specific fluorescence the 2.5th percentile of the *Aureobasidium* cell population. This is the same as saying that there is a 2.5% chance that a randomly selected *A. pullulans* cell will be declared non-*Aureobasidium*. If fluorescence in the *Aureobasidium* population were normally distributed (which it is not; Fig. 14), then this limit would be formally equivalent to the lower bound of the standard 95% confidence limits (mean ± 2 standard deviations). This threshold was set based on the generally accepted statistical (95%) precedent and our anticipated use of probe Ap665 to study the demography of *A. pullulans* on apple leaves.

At the 2.5th percentile level, there was no overlap between the controls and the distribution of cells hybridized with Ap665 (Fig. 14). However, in a population of 1,412 *Aureobasidium* cells examined, by definition setting a 2.5% level implies attributing the 35 dimmest cells to *Cryptococcus*. (Because mechanical categorization or binning of fluorescing cells is discrete, the actual number at the nearest bin may be more than the mathematical percentage.) Conversely, with the 2.5th-percentile bound, 34 of 817 (4.2%) *Cryptococcus* cells hybridized

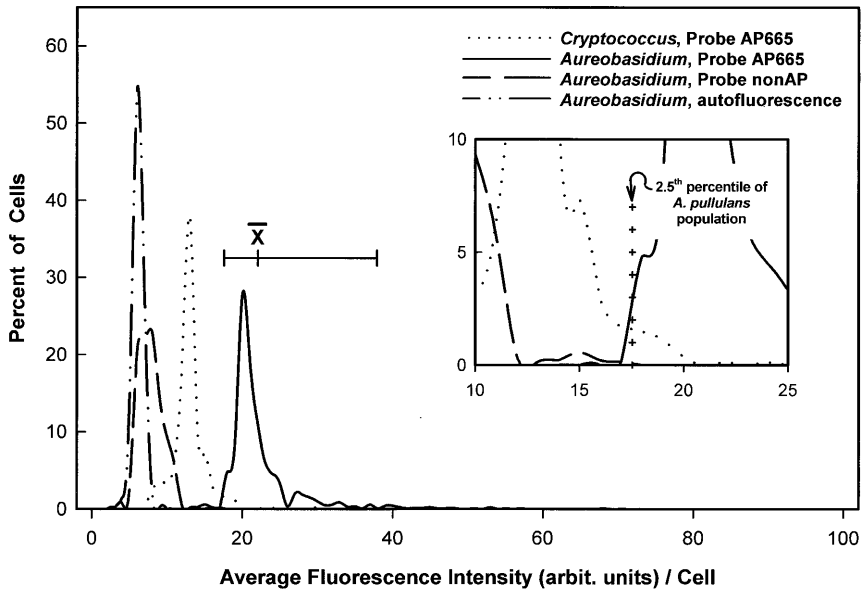

FIG. 14. Fluorescence intensity distribution for the following cell populations (total cell numbers for each are in parentheses): *C. laurentii* with probe Ap665 (817); *Aureobasidium* with probe Ap665 (1,412); *Aureobasidium* with probe non-Ap665 (1,445); *Aureobasidium* autofluorescence (623). The mean ($\bar{X}$) and limits of the fluorescence intensity distribution for 95% of the *Aureobasidium* cells hybridized with probe Ap665 are shown. The zone of overlap with the *Cryptococcus* population is enlarged (inset), and the 2.5th-percentile boundary is indicated by the vertical plus signs. As reference points for comparison with the semiquantitative scale (see footnotes for Table 1) of − to ++++, the fluorescence intensity distributions per cell corresponded as follows: *Aureobasidium* autofluorescence, −; *Aureobasidium*, probe non-Ap665, − to −/+; *Cryptococcus*, probe non-Ap665, −/+ to +; *Aureobasidium*, probe Ap665, + to ++++; $\bar{X}$, ++++. Arbit., arbitrary.

with Ap665 sufficiently brightly to be declared *Aureobasidium*. If the lower boundary is set instead at the 5th-percentile level, the respective numbers are 70 *Aureobasidium* cells "lost" but only 17 *Cryptococcus* cells "gained." Depending on the population distribution and the limits chosen, errors attributable to inclusion or exclusion may more or less balance. Overall, in this example, it makes more sense to set the bounds at the 2.5th- than the 5th-percentile level. Further discrimination between nonspecific and specific signals can probably be achieved by changing the stringency of the posthybridization washes. Depending on their objectives, other researchers may opt to set limits based on other criteria and to weigh inherent tradeoffs differently. In practice, populations of heterologous phyllosphere fungi would need to be monitored during the season and tested separately on slides, as was done here, for their hybridization signal distribution relative to *Aureobasidium*, and the boundary would need to be set or readjusted based on tolerable overlap according to the protocol identified above.

We conclude that quantitative FISH can be used in studies of the population biology of *A. pullulans* from laboratory culture and, more significantly, on leaf surfaces in nature. While our results were consistent and often striking with plant material from growth chambers, some progressive deterioration in signal quality occurred with field samples over time, beginning in mid-late season and persisting until leaf abscission. This was due apparently to changes in the autofluorescence characteristics of leaves as they age, together with the release of extractable compounds into the fixative and hybridization solutions. Our preliminary studies (data not shown) on different sources and ages of leaf material and reconstruction experiments in which *A. pullulans* cells were processed for hybridization with and without leaf material and then applied to microscope slides or different sources of leaves, showed that the extracted chemicals can impart a yellow-orange fluorescence to the fungal cells (which normally have a dull tan autofluorescence). This change shifted the FITC signal from bright green to yellow or yellow-orange. Judging from the amber color imparted to the processing solutions by older field leaves and the prevalence of phenolics in apple tissue (32, 41), we speculate that the compounds responsible may be phenolics, whose fluorescent properties are well recognized (28). The autofluorescence of field leaves, though variable and to some degree fixative dependent, ranged from tan to orange-red and intensified with time. The net effect of these separate but concurrent age-related processes was a decrease in the signal/noise ratio. Further studies of this phenomenon, particularly of the chemical nature of the extractable materials and ways to overcome the problem, are in progress. These effects undoubtedly will be shown to vary with plant source, among other factors, and could be inconsequential in many situations. Nevertheless, they pose a cautionary note for phylloplane researchers and may influence the utility of FISH in some circumstances.

To our knowledge this is the first application of FISH in phyllosphere research and also its first application to fungal populations in an ecological context. The utility of the method is apparent, and it should be especially powerful when combined with confocal microscopy to overcome topographic limitations and image analysis to quantify signal distribution or a microbial population of interest within a community. The in situ aspect of FISH will be valuable wherever it is desirable to retain microbe-to-substratum spatial information. Cases in point are phyllosphere and rhizosphere studies where there are many microhabitats (5, 9) and where a knowledge of microenvironmental relationships is important in understanding the colonization process.

ACKNOWLEDGMENTS

This research was supported in part by grants R81-9377 and R82-3845 to J.H.A. from the U.S. Environmental Protection Agency-National Center for Environmental Research and Quality Assurance.

We thank N. R. Pace, D. A. Stahl, and G. S. Wickham for suggestions and encouragement; CLONTECH Laboratories for the multifluorescein probes; R. Caldwell for assistance with culturing the fungi; D. Sonneborn for *Blastocladiella* cultures; E. Nordheim for discussions on statistics; C. Laper for technical assistance; and W. Hickey for comments on the manuscript.

REFERENCES

1. **Amann, R. I.** 1995. Fluorescently labelled, rRNA-targeted oligonucleotide probes in the study of microbial ecology. Mol. Ecol. **4:**543–554.
2. **Amann, R. I., L. Krumholz, and D. A. Stahl.** 1990. Fluorescent-oligonucleotide probing of whole cells for determinative, phylogenetic, and environmental studies in microbiology. J. Bacteriol. **172:**762–770.
3. **Amann, R. I., W. Ludwig, and K.-H. Schleifer.** 1995. Phylogenetic identification and in situ detection of individual microbial cells without cultivation. Microbiol. Rev. **59:**143–169.
4. **Amann, R. I., B. J. Binder, R. J. Olson, S. W. Chisholm, R. Devereux, and D. A. Stahl.** 1990. Combination of 16S rRNA-targeted oligonucleotide probes with flow cytometry for analyzing mixed microbial populations. Appl. Environ. Microbiol. **56:**1919–1925.
5. **Andrews, J. H.** 1992. Biological control in the phyllosphere. Annu. Rev. Phytopathol. **30:**603–635.
6. **Andrews, J. H., F. M. Berbee, and E. V. Nordheim.** 1983. Microbial antagonism to the imperfect stage of the apple scab pathogen *Venturia inaequalis*. Phytopathology **73:**228–234.
7. **Andrews, J. H., R. F. Harris, R. N. Spear, G. W. Lau, and E. V. Nordheim.** 1994. Morphogenesis and adhesion of *Aureobasidium pullulans*. Can. J. Microbiol. **40:**6–17.
8. **Assmus, B., P. Hutzler, G. Kirchhof, R. Amann, J. R. Lawrence, and A. Hartmann.** 1995. In situ location of *Azospirillum brasilense* in the rhizosphere of wheat with fluorescently labeled, rRNA-targeted oligonucleotide probes and scanning confocal laser microscopy. Appl. Environ. Microbiol. **61:**1013–1019.
9. **Beattie, G. A., and S. E. Lindow.** 1995. The secret life of foliar bacterial pathogens on leaves. Annu. Rev. Phytopathol. **33:**145–172.
10. **Bertin, B., O. Broux, and M. Van Hoegaerden.** 1990. Flow cytometric detection of yeast by *in situ* hybridization with a fluorescent ribosomal RNA probe. J. Microbiol. Methods **12:**1–12.
11. **Brelje, T. C.** 1996. Confocal Assistant, version 3.10, a shareware program for manipulating Bio-Rad confocal images. Available on the Internet from ftp://ftp.genetics.bio-rad.com/public/confocal/cas/CAS3.10.ZIP. Department of Cell Biology and Neuroanatomy, University of Minnesota Medical School, Minneapolis, Minn.
12. **Caldwell, D. E., D. R. Korber, and J. R. Lawrence.** 1992. Confocal laser microscopy and digital image analysis in microbial ecology. Adv. Microb. Ecol. **12:**1–67.
13. **Chen, H., J. R. Swedlow, M. Grote, J. W. Sedat, and D. A. Agard.** 1995. The collection, processing, and display of digital three-dimensional images of biological specimens, p. 197–210. *In* J. B. Pawley (ed.), Handbook of biological confocal microscopy. Plenum Press, New York, N.Y.
14. **Cooke, W. B.** 1959. An ecological life history of *Aureobasidium pullulans* (de Bary) Arnaud. Mycopathol. Mycol. Appl. **21:**225–271.
15. **De Hoog, G. S., and N. A. Yurlova.** 1994. Conidiogenesis, nutritional physiology and taxonomy of *Aureobasidium* and *Hormonema*. Antonie Leeuwenhoek **65:**41–54.
16. **DeLong, E. F., G. S. Wickham, and N. R. Pace.** 1989. Phylogenetic stains: ribosomal RNA-based probes for the identification of single cells. Science **243:**1360–1363.
17. **Drahos, D. J.** 1991. Methods for the detection, identification, and enumeration of microbes, p. 135–157. *In* J. H. Andrews and S. S. Hirano (ed.), Microbial ecology of leaves. Springer-Verlag, New York, N.Y.
18. **Giovannoni, S. J., E. F. DeLong, G. J. Olsen, and N. R. Pace.** 1988. Phylogenetic group-specific oligodeoxynucleotide probes for identification of single microbial cells. J. Bacteriol. **170:**720–726.
19. **Haugland, R. P.** 1996. Handbook of fluorescent probes and research chemicals, 6th ed. Molecular Probes Inc., Eugene, Oreg.
20. **Humanson, G. L.** 1972. Animal tissue techniques, 3rd ed. W. H. Freeman, San Francisco, Calif.
21. **Langendijk, P. S., F. Schut, G. J. Jansen, G. C. Raangs, G. R. Kamphuis, M. H. F. Wilkinson, and G. W. Welling.** 1995. Quantitative fluorescence in situ hybridization of *Bifidobacterium* spp. with genus-specific 16S rRNA-targeted probes and its application in fecal samples. Appl. Environ. Microbiol. **61:**3069–3075.
22. **Leitch, A. R., T. Schwarzacher, D. Jackson, and I. J. Leitch.** 1994. *In situ* hybridization: a practical guide. Bios Scientific Publishers, Oxford, United Kingdom.
23. **Li, S., C. P. Harris, and S. A. Leong.** 1993. Comparison of fluorescence *in situ* hybridization and primed *in situ* labeling methods for detection of single-copy genes in the fungus *Ustilago maydis*. Exp. Mycol. **17:**301–308.
24. **Li, S., R. Spear, and J. H. Andrews.** 1994. Detection and quantification of fungal cells on leaves by *in situ* hybridization based on 18S rRNA-targeted fluorescent oligonucleotide probes, p. 125. *In* Abstracts of the Fifth International Mycological Congress, Vancouver, Canada. Mycological Society of America, Lawrence, Kans.
25. **Li, S., R. Spear, and J. H. Andrews.** 1996. Detection and quantification of the fungus *Aureobasidium pullulans* on leaves by *in situ* hybridization with multifluorescein-labelled oligonucleotide probes. Phytopathology **86:**S12. (Abstract.)
26. **Li, S., D. Cullen, M. Hjort, R. Spear, and J. H. Andrews.** 1996. Development of an oligonucleotide probe for *Aureobasidium pullulans* based on the small-subunit rRNA gene. Appl. Environ. Microbiol. **62:**1514–1518.
27. **Lim, E. L., D. A. Caron, and E. F. DeLong.** 1996. Development and field application of a quantitative method for examining natural assemblages of protists with oligonucleotide probes. Appl. Environ. Microbiol. **62:**1416–1423.
28. **O'Brien, T. P., and M. E. McCully.** 1981. The study of plant structure: principles and selected methods. Termarcarphi Pty., Melbourne, Australia.
29. **Optimas Corp.** 1995. Optimas 5 user guide and technical reference, vol. 1. Optimas Corp., Bothell, Wash.
30. **Parkinson, D., and D. C. Coleman.** 1991. Microbial communities, activity and biomass. Agric. Ecosyst. Environ. **34:**3–33.
31. **Poulsen, L. K., G. Ballard, and D. A. Stahl.** 1993. Use of rRNA fluorescence in situ hybridization for measuring the activity of single cells in young and established biofilms. Appl. Environ. Microbiol. **59:**1354–1360.
32. **Pridham, J. B. (ed.).** 1960. Phenolics in plants in health and disease. Pergamon Press, Oxford, United Kingdom.
33. **Shaw, P. J.** 1995. Comparison of wide-field/deconvolution and confocal microscopy for 3D imaging, p. 373–387. *In* J. W. Pawley (ed.), Handbook of biological confocal microscopy, 2nd ed. Plenum Press, New York, N.Y.
34. **Soll, D. R., R. Bromberg, and D. R. Sonneborn.** 1969. Zoospore germination in the water mold, *Blastocladiella emersonii.* I. Measurement of germination and sequence of subcellular morphological changes. Dev. Biol. **20:**183–217.
35. **Stahl, D. A., and R. Amann.** 1991. Development and application of nucleic acid probes, p. 205–248. *In* E. Stackebrandt and M. Goodfellow (ed.), Nucleic acid techniques in bacterial systematics. John Wiley & Sons, New York, N.Y.
36. **Tkachuk, D. C., D. Pinkel, W.-L. Kuo, H.-U. Weier, and J. W. Gray.** 1991. Clinical applications of fluorescence *in situ* hybridization. Genet. Anal. Tech. Appl. **8:**67–74.
37. **Trask, B.** 1991. Fluorescence *in situ* hybridization: applications in cytogenetics and gene mapping. Trends Genet. **7:**149–154.
38. **Uzawa, S., and M. Yanagida.** 1992. Visualization of centromeric and nucleolar DNA in fission yeast by fluorescence *in situ* hybridization. J. Cell Sci. **101:**267–275.
39. **Wallner, G., R. Amann, and W. Beisker.** 1993. Optimizing fluorescent *in situ* hybridization with rRNA-targeted oligonucleotide probes for flow cytometric identification of microorganisms. Cytometry **14:**136–143.
40. **White, N. S.** 1995. Visualization systems for multidimensional CLSM images, p. 211–254. *In* J. W. Pawley (ed.), Handbook of biological confocal microscopy, 2nd ed. Plenum Press, New York, N.Y.
41. **Williams, A. H.** 1957. The simpler phenolic substances of plants. J. Sci. Food Agric. **8:**385–389.